

NUMERICAL INVESTIGATION ON SERPENTINE FLOW FIELD AND RHOMBUS ELECTROLYTE COMPARTMENT OF VANADIUM REDOX FLOW BATTERY (V-RFB)

A. C. Khor¹, M. R. Mohamed¹, M. H. Sulaimen¹, H. Daniyal¹, A.N. Oumer², P. K. Leung³

¹Sustainable Energy & Power Electronics Research Cluster (SuPER), Faculty of Electrical & Electronics Engineering, ²Universiti Malaysia Pahang 26600 Pekan, Pahang, Malaysia.

³Instituto IMDEA Energía, Avda. Ramón de la Sagra, 3, Parque Tecnológico de Móstoles, E-28935 Móstoles, Madrid, Spain
*corresponding author: rusllim@ump.edu.my

ABSTRACT

Selection of suitable material, fitting for prototype design and pumping rates are three affecting element for cost effectiveness and improve performance of vanadium cell prototype investigation. Therefore, three-dimensional numerical model isothermal computational fluid dynamics (CFD) model of vanadium redox flow battery (V-RFB) is studied. In this work, V-RFB with different electrolyte compartments is proposed and the effect of serpentine flow field is investigated. The performance of two V-RFBs with diamond and square electrolyte compartment is numerically tested. This work has been performed to optimize flow rate, electrolyte compartment design, avoid stagnant fluid and flow field application in V-RFB. For the simulation, the flow was assumed to be incompressible, isothermal, steady state flow, laminar and Newtonian flow. Results show that the application of flow field and Rhombus type electrolyte compartment can facilitate the distribution of electrolyte in the unit cell uniformity and avoid stagnant in the tank. Simulation results indicate the diamond shape and serpentine flow field at optimal flow rate show the most suitable for V-RFBs than square shape.

Keywords: Numerical investigation, Serpentine flow plate, Vanadium redox flow cell

INTRODUCTION

With the exhausted development of crude oil energy generation, the researchers have shifted their attention toward renewable energy generation and targeted zero carbon consumption technology for smart cities application. However, the intermittent of wind and solar energy make renewable energy less attached to the supply to meet the demand. Therefore, energy storage efficient technology like redox cell is needed with advantages of low carbon emission, long lifespan, scalable and decouples power and capacity. Examples of this technology include Zinc/bromide, iron/chromium, polysulphine/bromide and all vanadium which has already apply for peak shaving, frequency regulation, load shifting and power quality control application [1]. However, full commercialization of all vanadium redox technology into market still faces different technological limitations. Limitations such as cost effectiveness, cell durability, thermal management and degradation of vanadium redox flow battery system are those concerns that addressed. In order to tackle these limitations, detailed approach involving experimental research effort and investment has to be significantly applied and performed. Referring to Xu *et al.*, the work shows the serpentine flow field application is the best compare to parallel and optimum flow rate selection is necessary for V-RFB[2].

To develop the V-RFB technologies, models for V-RFB are crated and validated with software and hardware. Modeling and simulation drive development of commercialization of V-RFB, excessive laboratory hardware testing of different material, operating parameter and methods are time consuming and non-cost effective. For the primary effort to construct laboratory test, systematically modeling can be used to reduce unnecessary test cases. One of the efforts is flow simulation; it is a part of the valuable step to ensure the designed V-RFB operation and provide valuable insight for the suitable material selection. Lots of simulation has

been done on PEM fuel cell, but only little attention was paid on V-RFB which very least technical data release and publish, which are useful for fabrication of large capacity V-RFB system. By referring to Iranzo *et al.* on his work, in his major work [3-6]involving CFD simulation for PEM fuel cell has become the major references for this simulation. Oh *et al.* used CFD modeling on three dimensional all-vanadium redox flow batteries shows model prediction and experimental data comparison to determine the optimal design and operating conditions[7].

Computational Fluid Dynamics (CFD) modelling is used as a tool to understand the detailed interaction between all the related factors such flow geometry, fluid dynamics, heat transfer and electrochemical in the cell . This software allows researchers to gain further insight on the structure applied to redox battery to perform design optimization. In this work, the aims from simulation are to check the pressure happen around the inlet and outlet and the distribution of electrolyte in the battery model. The outcome of the simulation would allow the suitable fitting to be applying during the battery model construction. By applying flow simulation on the designed model, researcher tend to figure out which flow field is the best to apply for the system instead of fabricate all of them for hardware experimental purpose.

In this work, the aims to be achieved from simulation are to check the pressure happen around the inlet and outlet, and the distribution of electrolyte in the battery model. The outcome of the simulation would allow the suitable fitting to be applied during construction of the model of the battery. By applying flow simulation on the designed model, instead of fabrication all of the models for hardware experimental purposes, researchers could figure out which flow field is the best to be applied to the system.

RELATED WORK

In this section, numerical model was developed for investigation with different parameter (i.e. flow field

application and flow rates) applied on rhombus and square electrode compartment.

NUMERICAL MODEL DEVELOPMENT

To perform the numerical simulation, the physical domain of a complete three dimensional electrochemical-thermal model for a V-RFB cell is drawn. For this simulation, as shown in Figure-1, a redox flow battery cell which consists of two cell plates, two current collectors, two carbon felt gaskets and two carbon serpentine flow plate was generated as shown in Figure-1. A total of 110.25 cm² acrylic polymer cell stack body is considered in the simulation. The parameter and specification such as reservoir volume, porous layer and cell frame dimension are presented in Table-2.

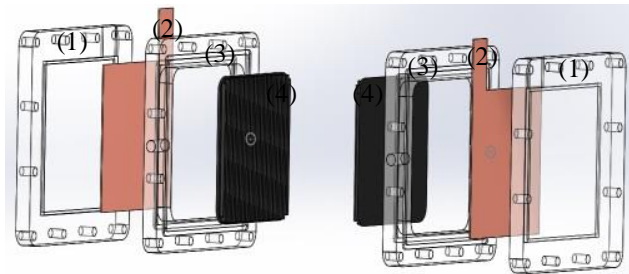


Figure-1 The V-RFB cell flow compartment: 1. cell plate; 2. current collector (copper); 3. carbon felt gasket; 4. carbon serpentine flow channel

Table-1 Specification of a laboratory V-RFB single unit cell

	Parameter
Cell stack body	Acrylic polymer
Electrode compartment	110.25 cm ²
Cell frame dimension	14.5 cm x 14.5 cm x 1.2 cm
Opening	10.5 cm x 10.5 cm
Porous layer	Carbon felt electrode (Sigratherm GFA5) with effective porosity 0.68 ± 0.07
Reservoir volume	250 ml

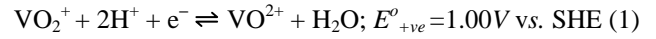
The two carbon plates have two serpentine with 24 channels each plate, shown in Figure-2. Each Channel has a width of 0.2 cm, length of 10.0 cm and depth of 0.2 cm. The fluid which circulates through the channels is vanadyl sulphate.

Table-2 lists the value of parameters for the simulation, including the physical properties of the material (density, specific heat, thermal conductivity). This parameter is used in the numerical simulation for V-RFB compartment investigation.

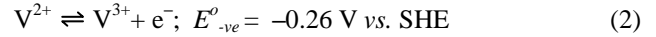
CHEMICAL REACTION IN V-RFB

The electrolyte used in the battery is a mixture of 250 ml electrolyte with 1: 1 ratio of V³⁺ ion and V⁴⁺ ion at 1.6 mol dm⁻³ dissolved in 4 mol dm⁻³ H₂SO₄. The homogeneous catalytic reactions that occurs at the interface of the electrode and electrolyte both in the negative and positive electrodes during discharge/charge states are shown below,

Positive electrode:



Negative electrode:



Overall cell reaction:



Note: VO²⁺ ≡ V⁴⁺; VO₂⁺ ≡ V⁵⁺

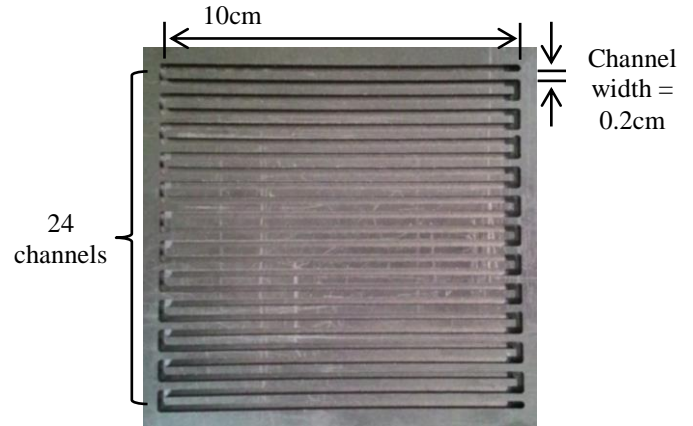


Figure-2 Bipolar plate with 24 channels; Channel width is 0.2 cm; length is 10.0 cm and depth of 0.2 cm

Table-2 Parameter values for the simulation

Parameters	Value
Carbon density	2.24 g cm ⁻³
Thickness of the cell wall	1.2 cm
Specific heat of carbon, Cp	0.71 J g ⁻¹ K ⁻¹
Thermal conductivity of carbon	0.20 W m ⁻¹ K ⁻¹
Vanadium Concentration, c	1.5 mol
Temperature, K	298.15
Specific heat of electrolyte, Cp	3.2 J g ⁻¹ K ⁻¹
Electrolyte dynamic viscosity	2.4 cP
Kinematic viscosity	3.2 cSt
Electrolyte density, ρ	1.3349 g cm ⁻³
Thermal conductivity of electrolyte	0.67 W m ⁻¹ K ⁻¹
Volume of the cell, V _c	0.25 L x 2 = 0.5 L
Membrane	Nafion 117
Thermal conductivity of membrane	0.13 W m ⁻¹ K ⁻¹

FLOW GOVERNING EQUATION

The flow is assumed to be incompressible, isothermal, steady state and laminar. Therefore, based on these assumptions the governing equations used in the simulation are continuity and momentum equations.

$$\nabla \cdot \overline{\rho \vec{v}} = 0 \quad (4)$$

where ρ is fluid density and \vec{v} is the fluid velocity.

$$\nabla \cdot \overline{\vec{v} \vec{v}} = -\nabla P + \nabla \cdot \tau + \rho g \quad (5)$$

where P is pressure, τ is viscous shear stress and g is gravity.

Other assumptions including additional existing species are ignored in this simulation and the evolution of nitrogen and oxygen are ignored. The operating pressure is set to be 101325 Pascal (stored as default value).

Without Flow Field:

For simulations without the flow channels, the pressure drop can be considered by Darcy's law:

$$\Delta p = \rho \frac{V}{K_p} \vec{u} \quad (6)$$

where K_p is the permeability coefficient that can be calculated according to the Kozeny-Carmen equation as below:

$$K_p = \frac{D_f^2 \varepsilon^3}{K_{ck}(1-\varepsilon)^2} \quad (7)$$

where D_f is defined as the mean fiber diameter of the electrode, ε is the porosity of graphite felt electrode, K_{ck} is the Carman-Kozeny constant for the fibrous medium. The flow pattern refers to design in Figure 5.2.

With Flow Field:

For simulation with the flow channels, the pressure drop through the electrode can be calculated as follows:

$$\Delta p = \rho \frac{V}{K_p A} \vec{u} \quad (8)$$

where \vec{u} is the flow rate in porous electrodes of each cell,

A is the characteristic area of electrode with distribution channel on the surface, which can be expressed as follows:

$$A = (w_c + w_r) \theta_\varepsilon \quad (9)$$

where w_c and w_r are respectively the widths of distribution channel and rib, and θ_ε is the thickness of the porous electrode.

The pressure drop through the distribution channels has two sources: fiction pressure drop and sudden change of fluid direction or velocity. Shear stress from the wall-fluid interface with viscous fluid cause friction pressure drop. The pressure drop through the channel is described as:

$$\Delta p_c = \left(f_c \frac{L_c}{D_{hc}} + K_{foam} \right) \frac{\rho}{2A_c^2} Q_c^2 \quad (10)$$

GEOMETRY AND MESH GENERATION

Two geometries with different electrolyte compartment were considered: rhombus shape and square shape. A mesh triangle was generated, and the elements were set to be 0.001m. Figure 5.4 shows a general view of

the 3D mesh and cross section of V-RFB cell. The temperature is set to room temperature which is 298.15 K.

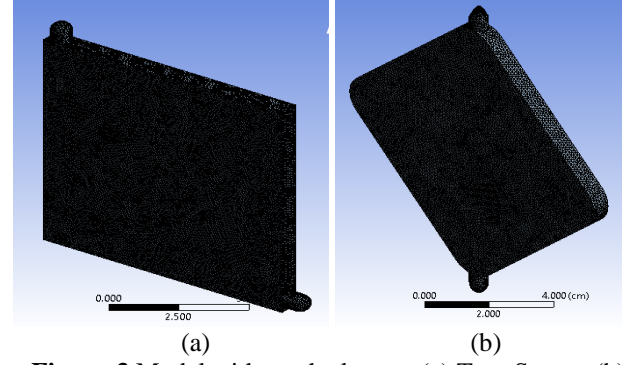


Figure-3 Model with mesh element (a) Top: Square (b) Bottom: Rhombus

$$\text{Mean velocity of fluid, } V_{in} = \frac{Q_e}{\varepsilon A} \quad (14)$$

Where V_{in} = mean velocity of electrolyte
 Q_e = volumetric flow rates of fluid (m^3/s)
 εA = total area (m^2)

Varied volumetric flow rates of fluid are applied to this work, which is $10 \text{ cm}^3 \text{ s}^{-1}$, $20 \text{ cm}^3 \text{ s}^{-1}$, $30 \text{ cm}^3 \text{ s}^{-1}$, $40 \text{ cm}^3 \text{ s}^{-1}$ and $50 \text{ cm}^3 \text{ s}^{-1}$ with the inlet tube having a diameter of 3mm. The flow rate for the initial simulation is set to be $10 \text{ cm}^3 \text{ s}^{-1}$ flowing in the y-direction.

$$N_R = \frac{V_{in} D_f}{\nu_k} \quad (15)$$

Where N_R = Reynolds number
 D_f = Diameter of pipe (m)
 ρ = Density of electrolyte (kg/m^3)
 ν_k = Kinematic viscosity (m^2/s)

BOUNDARY CONDITIONS

The boundary conditions were defined to set the operating point of V-RFB cell which includes the velocity of the electrolyte into inlets, pressure outlet, symmetry planes and wall condition of the battery surfaces. Figure- 4 illustrates all the boundary conditions. No-slip condition (zero velocity) and no flux condition are applied to the external surfaces of the computational domain except for the inlets and outlets.

The mass velocity and electrolyte species are prescribed at the inlet. The flow is presumed uniform for the velocity field. To evaluate the pressure field, the pressure-velocity coupling algorithm SIMPLE (Semi Implicit Method for Pressure-Linked Equation) was selected. Velocity condition for the inlets and pressure condition for the outlets are used. The boundary conditions can be specified by referring to Figure-4 as follows:

Y_1 = inlet (velocity), Y_2 = liquid (interface), Y_3 = outlet (pressure)

At the inlet:

$$\vec{u} = \vec{u}_0$$

At the outlet:

$$P = P_{out}$$

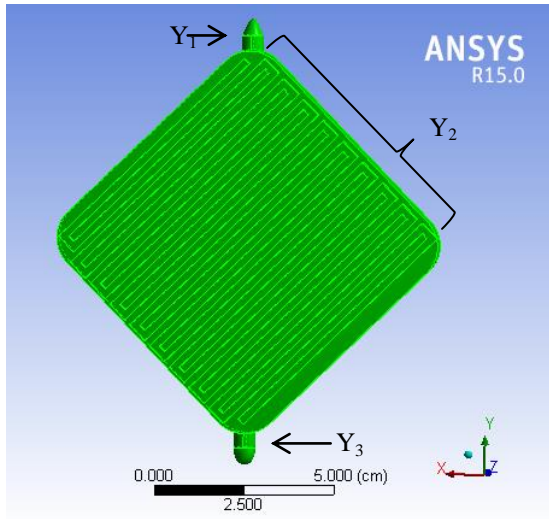


Figure-4 Applied boundary conditions

RESULT AND DISCUSSION

Cell flow rates

The model has been validated using numerical investigation and presented in Figure-5 to Figure-9. The figures display the evolution of total pressure contour and electrolyte distribution in battery cell for each flow rate. Different flow rates ranging from $10 \text{ cm}^3 \text{ s}^{-1}$ to $50 \text{ cm}^3 \text{ s}^{-1}$ have been applied after referring [2], to the half unit cell to detect the pressure acting on the cell and check the suitable flow rate for better distributed electrolyte solution in the cell.

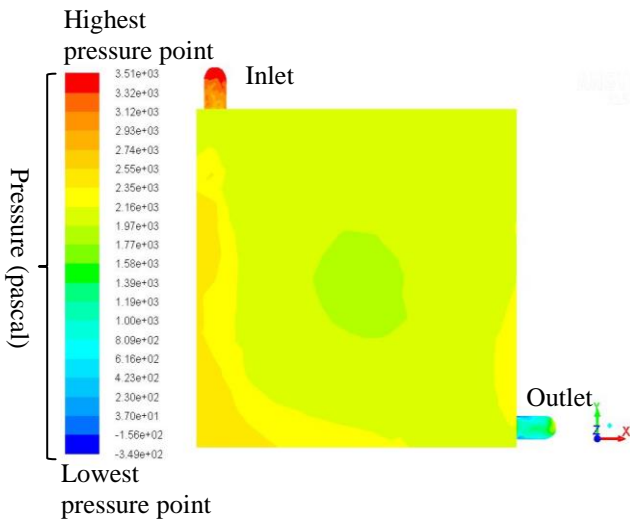


Figure-5 Evolution of total pressure contour and electrolyte distribution for volumetric flow rate ($10 \text{ cm}^3 \text{ s}^{-1}$)

For $10 \text{ cm}^3 \text{ s}^{-1}$ flow rate, laminar flow has been applied toward the reactive area, while the optimum electrolyte flow rate lies between of $10 \text{ cm}^3 \text{ s}^{-1}$ to $50 \text{ cm}^3 \text{ s}^{-1}$. The maximum pressure suffer by inlet is 3.51×10^3 Pascal., located the optimum value for electrolyte flowing rate. The desired flow pattern with less pumping loss was desired for an effective battery system.

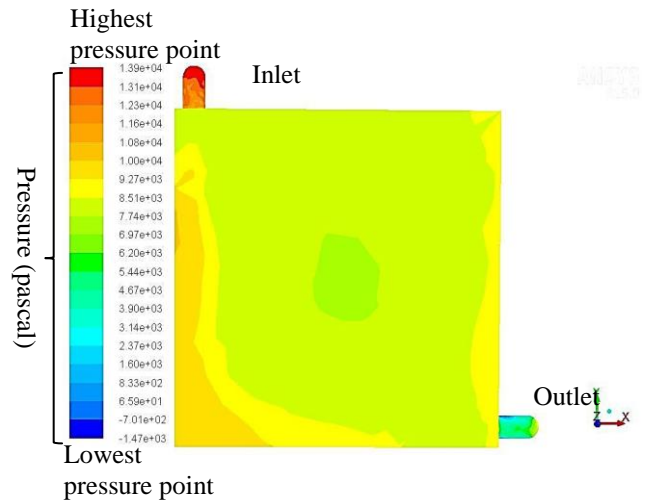


Figure-6 Evolution of total pressure contour and electrolyte distribution for volumetric flow rate ($20 \text{ cm}^3 \text{ s}^{-1}$)

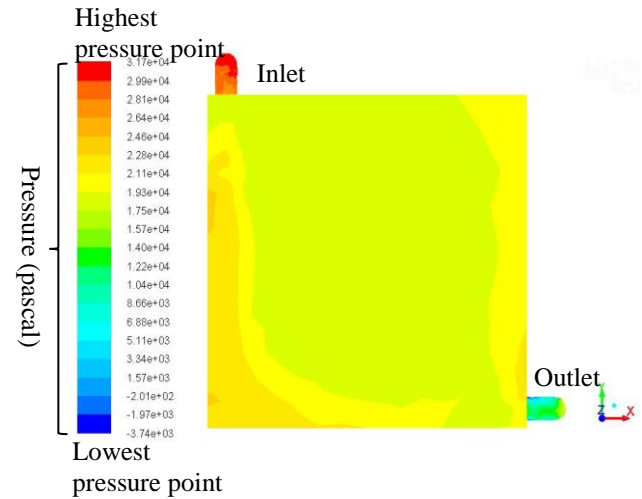


Figure-7 Evolution of total pressure contour and electrolyte distribution for volumetric flow rate ($30 \text{ cm}^3 \text{ s}^{-1}$)

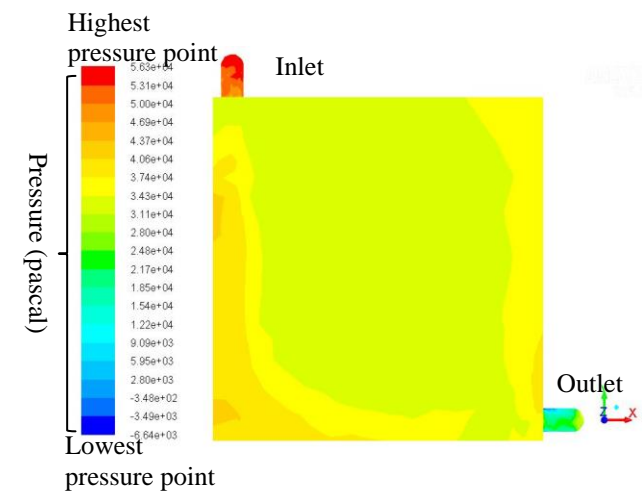


Figure-8 Evolution of total pressure contour and electrolyte distribution for volumetric flow rate ($40 \text{ cm}^3 \text{ s}^{-1}$)

Figure-5 until Figure-9 show the evolution for different volumetric flow rates starting from $30 \text{ cm}^3 \text{ s}^{-1}$ to $50 \text{ cm}^3 \text{ s}^{-1}$. The mean velocity and pressure increases linearly with the applied flow rates. The higher the flow rate, the higher the pressure and electrolyte velocity. According to Darcy's law, the pressure drop increases linearly with the velocity.

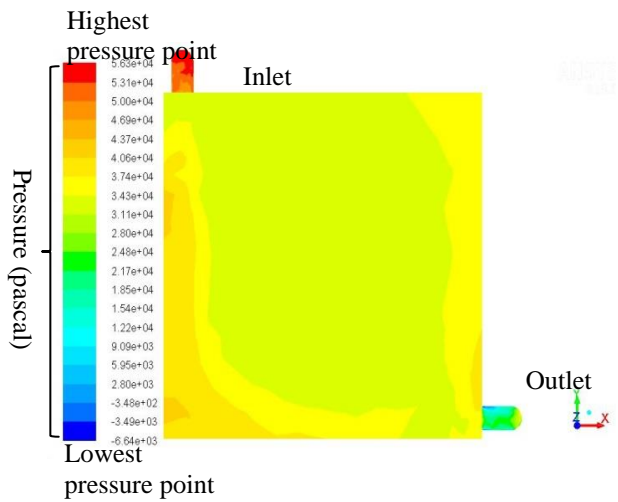


Figure-9 Evolution of total pressure contour and electrolyte distribution for volumetric flow rate ($50\text{cm}^3\text{ s}^{-1}$)

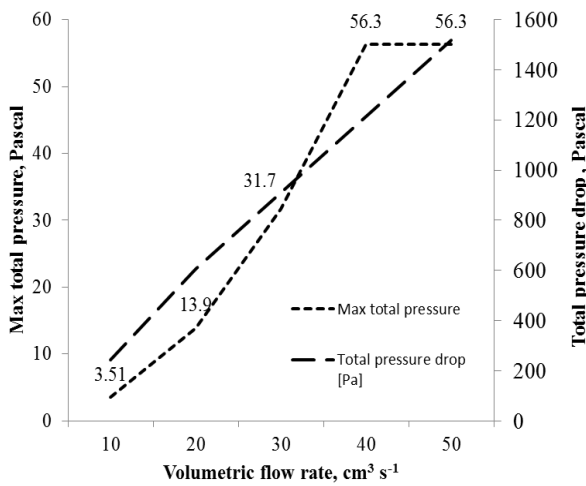


Figure-10 Volumetric flow rate versus max total pressure and total pressure drop suffer by the cell

Table-3 Calculated pressure drop for square type compartment

Volumetric flow rate [$\text{cm}^3\text{ s}^{-1}$]	Total pressure drop [Pa]
10	245.00
20	607.25
30	910.98
40	1214.71
50	1518.23

Table-3 shows the relationship of flow rates with calculated total pressure drop. Flow rates are directly proportional with total pressure drop, as display in the table.

Comparison between Rhombus and Square

From Figure-10, it is noted that the increase in volumetric flow rate also cause the total pressure in the cell to increase. High pumping loss will cause the loss for the complete system, which will increase the cost.

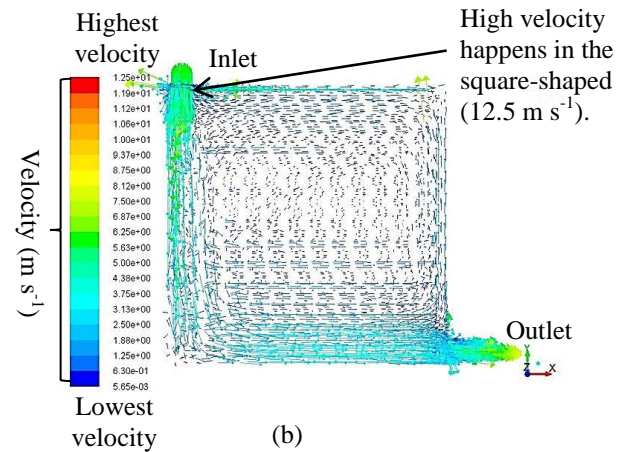
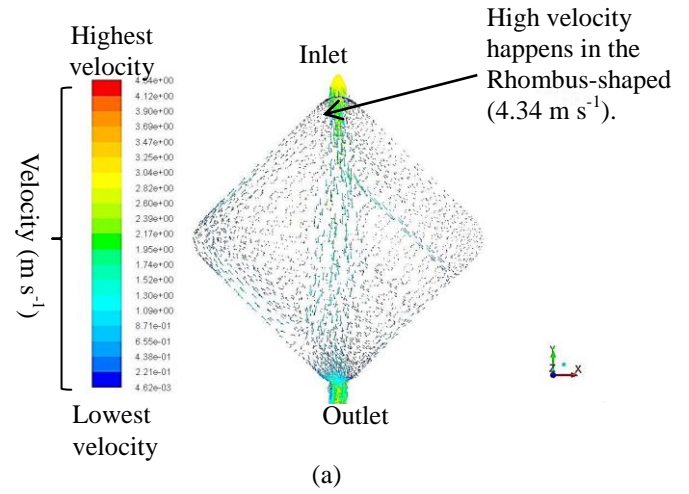


Figure-11 Comparison velocity magnitude vector between (a) rhombus shape and (b) square shape

Figure-11 shows the flow pattern for each design of the flow compartment. It is observed that the square-shaped compartment has higher velocity of (12.5 m s^{-1}) compared to that of the diamond-shaped compartment (4.34 m s^{-1}). The square-shaped compartment has a high possibility of the electrolyte being stagnant at the end of the left-hand corner of the compartment, as shown in region A. However, compared to the diamond-shaped compartment, the square-shaped compartment has better overflow as the push over of the electrolyte might reduce the possibility of stagnancy in the tank. In comparison, the diamond-shaped compartment provides a passive route to the electrolyte, which is theoretically good for the system to achieve the hydrostatic equilibrium.

Figure-12(b) shows the total pressure suffered by diamond-shaped and square-shaped electrolyte tank, respectively. In Figure-12(b), the pressure distribution is as follows: Region D < Region C < Region B < Region A < Region E. Figure-12(b) shows that, the highest pressure distribution is located in region E. The total pressure is an important parameter for selecting suitable flow rate and pumps for V-RFB system. The diamond-shaped compartment has a lower pressure (12.1kPa) compared to that of the square-shaped compartment (77.0kPa). According to the Bernoulli principle, it states that the highest the pressure the slowest the flow of liquid.

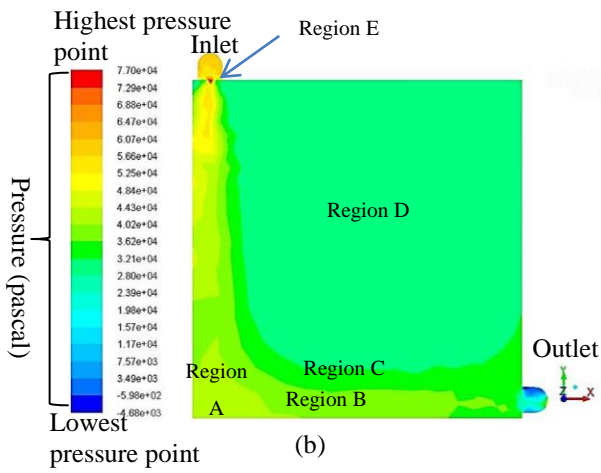
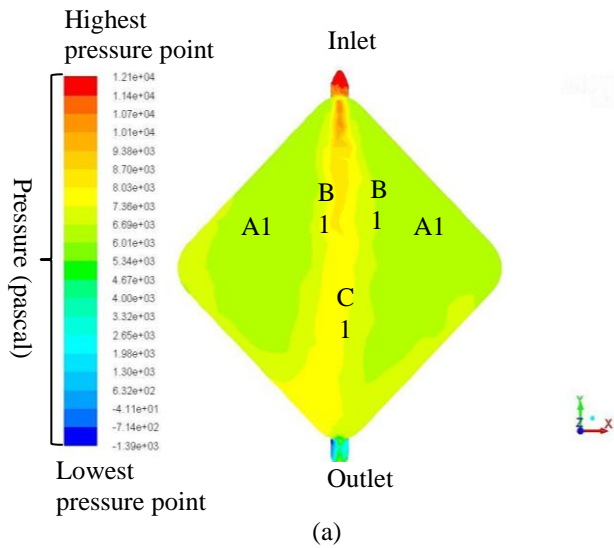


Figure-12 Comparison total pressure vector between (a) rhombus shape and (b) square shape

CONCLUSION

Based on the simulation, the fitting will be chosen with a safety factor of + 2 bars to withstand the pressure that might occur during the hardware operation. However, another factor which is the acidic composition in the vanadium solution should be considered as well during the selection of fitting material.

1. Issue- shunt current-prevalent
Problem of mass transfer and pumping losses of electrolytes can be very energy insufficient. Proposed flow rate for battery durability is expected to have lower gravimetric and volumetric power and energy densities than reversible fuel cell.
2. Hydrostatic pressure in the liquid deal with time independent state of fluids
3. Non-uniformelectrolytes for porous flow through electrode exist in unit cell, this flow phenomenon needs to be considered in stack design of V-RFB.
4. The performance of the battery is influenced by the design of flow pattern; flow field pattern can improve the distribution of electrolytes through the electrode and avoid stagnant happen in the compartment.

In this study, the diamond-shaped electrolyte tank suits better for V-RFB than the square-shaped electrolyte tank. The main contribution obtained from the study is that the optimum flow rate is found to be $30 \text{ cm}^3 \text{ s}^{-1}$; however, this model is carried out for a very minor part of V-RFB. Also, the influence of mixing the different species is not considered in the present model. Therefore, to obtain better and more accurate result prediction, a complete developed V-RFB model in CFD in terms of thermal modeling and electrical behavior will be needed to fully predict the behavior of V-RFB cell for better battery performance estimation.

ACKNOWLEDGEMENTS

This work was supported by Ministry of Education (MOE) Malaysia under research grant RDU 130802 and GRS 140329.

REFERENCES

- [1] H. D. Daniel, C. B. Paul, A. A. Abbas, H. C. Nancy, and D. B. John, "Batteries for large Scale Stationary Electrical Energy Storage," *The Electrochemical Society Interface*, pp. 49-53, 2010.
- [2] Q. Xu, T. S. Zhao, and P. K. Leung, "Numerical investigations of flow field designs for vanadium redox flow batteries," *Applied Energy*, vol. 105, pp. 47-56, 5// 2013.
- [3] A. Iranzo, M. Muñoz, J. Pino, and F. Rosa, "Update on numerical model for the performance prediction of a PEM Fuel Cell," *International Journal of Hydrogen Energy*, vol. 36, pp. 9123-9127, 7// 2011.
- [4] A. Iranzo, P. Boillat, P. Oberholzer, and J. Guerra, "A novel approach coupling neutron imaging and numerical modelling for the analysis of the impact of water on fuel cell performance," *Energy*, vol. 68, pp. 971-981, 4/15/ 2014.
- [5] A. Iranzo, P. Boillat, and F. Rosa, "Validation of a three dimensional PEM fuel cell CFD model using local liquid water distributions measured with neutron imaging," *International Journal of Hydrogen Energy*, vol. 39, pp. 7089-7099, 4/24/ 2014.
- [6] A. Iranzo, M. Muñoz, F. Rosa, and J. Pino, "Numerical model for the performance prediction of a PEM fuel cell. Model results and experimental validation," *International Journal of Hydrogen Energy*, vol. 35, pp. 11533-11550, 10// 2010.
- [7] K. Oh, H. Yoo, J. Ko, S. Won, and H. Ju, "Three-dimensional, transient, nonisothermal model of all-vanadium redox flow batteries," *Energy*, 2014.